

Resistance and resistance fluctuations in random resistor networks under biased percolation

C. Pennetta,^{1,*} L. Reggiani,¹ Gy. Trefán,² and E. Alfinito¹

¹*INFM - National Nanotechnology Laboratory, Dipartimento di Ingegneria dell'Innovazione, Università di Lecce, Via Arnesano, I-73100 Lecce, Italy*

²*Department of Electrical Engineering, Eindhoven University of Technology, 5600 MB Eindhoven, The Netherlands*

(Received 16 February 2002; published 24 June 2002)

We consider a two-dimensional random resistor network (RRN) in the presence of two competing biased processes consisting of the breaking and recovering of elementary resistors. These two processes are driven by the joint effects of an electrical bias and of the heat exchange with a thermal bath. The electrical bias is set up by applying a constant voltage or, alternatively, a constant current. Monte Carlo simulations are performed to analyze the network evolution in the full range of bias values. Depending on the bias strength, electrical failure or steady state are achieved. Here we investigate the steady state of the RRN focusing on the properties of the non-Ohmic regime. In constant-voltage conditions, a scaling relation is found between $\langle R \rangle / \langle R \rangle_0$ and V/V_0 , where $\langle R \rangle$ is the average network resistance, $\langle R \rangle_0$ the linear regime resistance, and V_0 the threshold value for the onset of nonlinearity. A similar relation is found in constant-current conditions. The relative variance of resistance fluctuations also exhibits a strong nonlinearity whose properties are investigated. The power spectral density of resistance fluctuations presents a Lorentzian spectrum and the amplitude of fluctuations shows a significant non-Gaussian behavior in the prebreakdown region. These results compare well with electrical breakdown measurements in thin films of composites and of other conducting materials.

DOI: 10.1103/PhysRevE.65.066119

PACS number(s): 64.60.Ak, 77.22.Jp, 07.50.Hp, 64.60.Fr

I. INTRODUCTION

The study of electrical and mechanical stability of disordered systems is attracting a considerable interest in the recent literature [1–23] because of its implications on both material technology [1,2,17–23] and fundamental aspects related to the response of these systems to high external stresses [1–16,24–26]. Indeed, the application of a finite stress (electrical or mechanical) to a disordered material generally implies a nonlinear response, which ultimately leads to an irreversible breakdown (catastrophic behavior) in the high stress limit [1–3,19]. Such catastrophic phenomena have been successfully studied by using percolation theories [1–7,11–16,23–37]. Critical phenomena near the percolation threshold have been widely investigated in the electrical breakdown of granular metals or conductor-insulator composites [1–7,12–16,24–37]. The associated critical exponents have been measured [1–3,6,16,25,26,30,31] and theoretically studied using continuum or lattice percolation models [1–3,25–37]. In particular, large attention has been devoted to the critical exponents describing the resistance and its relative noise in terms of the medium properties (e.g., conducting particle fraction, defect concentration, etc.) [1–6,16,25–37]. However, very few attempts [12–15,38,39] have been made so far to describe the behavior of a disordered medium over the full range of the applied stress, i.e., by studying the response of the system to an external bias when the bias strength covers the full range of linear and nonlinear regimes. Therefore, a satisfactory understanding of breakdown phenomena over the full dynamical regime is still missing [13,15]. On the other hand, relevant information can be obtained from such a study, like: precursor phenomena,

role of the disorder, existence of scaling laws, predictability of breakdown, etc. [1–3,13,15,24].

Here we present a model of sufficient generality to address the above issues. Our aim is to provide a theoretical framework to study response and fluctuation phenomena under linear and nonlinear regimes in a wide class of disordered systems. To this purpose, we study the evolution of a random resistor network (RRN) in which two competing processes are present, defect generation and defect recovery, which determine the values of the elementary network resistances. The two processes are biased percolations [34,38], i.e., driven by the joint effect of an electrical bias and of the heat exchange between the network and the thermal bath. The bias is applied through a constant voltage or, alternatively, a constant current. Monte Carlo (MC) simulations are performed to investigate the network evolution in the full range of bias values. Depending on the bias strength, an irreversible failure or a stationary state of the RRN can be achieved. By focusing on the steady state, we analyze the behavior of the average network resistance $\langle R \rangle$ and the properties of the resistance fluctuations as a function of the bias. In constant-voltage conditions, a scaling relation is found between $\langle R \rangle / \langle R \rangle_0$ and V/V_0 , where $\langle R \rangle_0$ is the linear regime resistance and V_0 the threshold value for the onset of nonlinearity. A similar relation is found in constant-current conditions. The relative variance of resistance fluctuations also exhibits a strong nonlinearity in the pre-breakdown regime whose properties are discussed. The fluctuation analysis is completed by a further investigation of the noise resistance spectrum and of the Gaussian features of the fluctuation amplitudes. Theoretical results agree with electrical breakdown measurements in thin films of composites [14,15] and of other conducting [17,20,40] or insulating materials [41].

The paper is organized as follows. In Sec. II we briefly describe the model used. Section III presents the results of

*Corresponding author. Email address: cecilia.pennetta@unile.it

the MC simulations for the resistance and its fluctuations. The main conclusions are drawn in Sec. IV.

II. MODEL

We study a two-dimensional random resistor network of total resistance R , made of N_{tot} resistors, each of resistance r_n , disposed on a square lattice. We take a square geometry, $N \times N$, where N determines the linear size of the lattice, with the total number of resistors being $N_{tot} = 2N^2$. For the comparison with resistivity measurements in thin films, the value of N can be related to the ratio between the size of the sample and the average size of the grains composing the sample. An external bias, represented by a constant voltage V or by a constant current I , is applied to the RRN through electrical contacts realized by perfectly conducting bars at the left- and right-hand sides of the network. A current i_n is then flowing through each resistor. The RRN interacts with a thermal bath at temperature T_0 and the resistances r_n are taken to depend linearly on the local temperatures, T_n , as

$$r_n(T_n) = r_0[1 + \alpha(T_n - T_0)]. \quad (1)$$

In this expression α is the temperature coefficient of the resistance and T_n is calculated by adopting the biased percolation model [34,36,37] as

$$T_n = T_0 + A \left[r_n i_n^2 + \frac{B}{N_{neig}} \sum_{l=1}^{N_{neig}} (r_l i_l^2 - r_n i_n^2) \right]. \quad (2)$$

Here, N_{neig} is the number of first neighbors around the n th resistor, the parameter A , measured in (K/W), describes the heat coupling of each resistor with the thermal bath and it determines the importance of Joule heating effects. The parameter B is taken to be equal to 3/4 to provide a uniform heating in the perfect network configuration. We note that Eq. (2) implies an instantaneous thermalization of each resistor at the value T_n , therefore, by adopting Eq. (2), for simplicity we are neglecting time dependent effects that are discussed in Ref. [32].

In the initial state of the network (corresponding to the perfect network configuration with no heating) all the resistors are identical: $r_n \equiv r_0$. Now, we assume that two competing processes act to determine the RRN evolution. The first process consists of generating fully insulating defects (resistors with very high resistance, i.e., broken resistors) with probability [34,36,37] $W_D = \exp(-E_D/K_B T_n)$, where E_D is an activation energy characteristic of the defect and K_B the Boltzmann constant. The second process consists of recovering the insulating defects with probability $W_R = \exp(-E_R/K_B T_n)$, where E_R is an activation energy characteristic of this second process [38]. Thus, the first process consists in a percolation of broken resistors within a network of active resistors. This percolative process is contrasted by the recovery process. This second process can also be seen as a percolation of active resistors within an insulating network. For $A \neq 0$, Eq. (2) implies that both the processes (defect generation and defect recovery) are correlated percolations. Indeed, the probability of breaking (recovering) a resistor is

higher in the so called ‘‘hot spots’’ of the RRN [25]. On the other hand, for $A=0$ Eq. (2) yields $T_n \equiv T_0$, which corresponds to random processes [25,42]. The same is true for vanishing small bias values, when Joule heating effects are negligible.

As a result of the competition between the two processes and depending on the parameters related to the particular physical system ($E_D, E_R, A, \alpha, r_0, N$) and on the external conditions (specified by the bias conditions and the bath temperature), the RRN reaches a steady state or exhibits an irreversible breakdown. In the first case, the network resistance fluctuates around an average value $\langle R \rangle$. In the second case, a critical fraction of defects p_c , corresponding to the percolation threshold, is reached, i.e., R diverges due to the existence of at least one continuous path of defects between the upper and lower sides of the network [25]. We note that in the limit of a vanishing bias (random processes) and infinite lattices ($N \rightarrow \infty$), the expression: $E_R < E_D + K_B T_0 \ln[1 + \exp(-E_D/K_B T_0)]$ provides a sufficient condition for the existence of a steady state [42].

The evolution of the RRN is obtained by MC simulations carried out according to the following iterative procedure. (i) Starting from the perfect lattice with given local currents, the local temperatures T_n are calculated according to Eq. (2); (ii) the defects are generated with probability W_D and the resistances of the unbroken resistors are changed as specified by Eq. (1); (iii) the currents i_n are calculated by solving Kirchhoff’s loop equations by the Gauss elimination method and the local temperatures are updated; (iv) the defects are recovered with probability W_R and the temperature dependence of unbroken resistors is again accounted for; (v) R , i_n , and T_n are finally calculated and the procedure is iterated from (ii) until one of the two following possibilities is achieved. In the first, the percolation threshold is reached. In the second, the RRN attains a steady state; in this case the iteration runs long enough to allow a fluctuation analysis to be carried out. Each iteration step can be associated with an elementary time step on an appropriate time scale (to be calibrated with experiments). In this manner it is possible to represent the simulation of the resistance evolution over either a time or a frequency domain according to convenience.

In the simulations, as reasonable values of the parameters, we have taken: $N=75$, $r_0=1 \Omega$, $\alpha=10^{-3} \text{ K}^{-1}$, $A=5 \times 10^5 \text{ K/W}$, $E_D=0.17 \text{ eV}$, $E_R=0.043 \text{ eV}$, and $T_0=300 \text{ K}$ if not stated otherwise. The values of the external bias range from $0.05 \leq I \leq 2.8 \text{ A}$ under constant-current conditions, and from $0.05 \leq V \leq 3.5 \text{ V}$ under constant-voltage conditions.

III. RESULTS

Figures 1(a) and 1(b) report a sampling of the resistance evolutions coming out from the simulations under steady-state conditions for the cases of constant voltage [Fig. 1(a)] and constant current [Fig. 1(b)], respectively. On increasing the external bias, a remarkable increase of the average resistance and of the amplitude of fluctuations is evident in both cases while approaching the breakdown. This is reached by applying an external bias just above the highest values

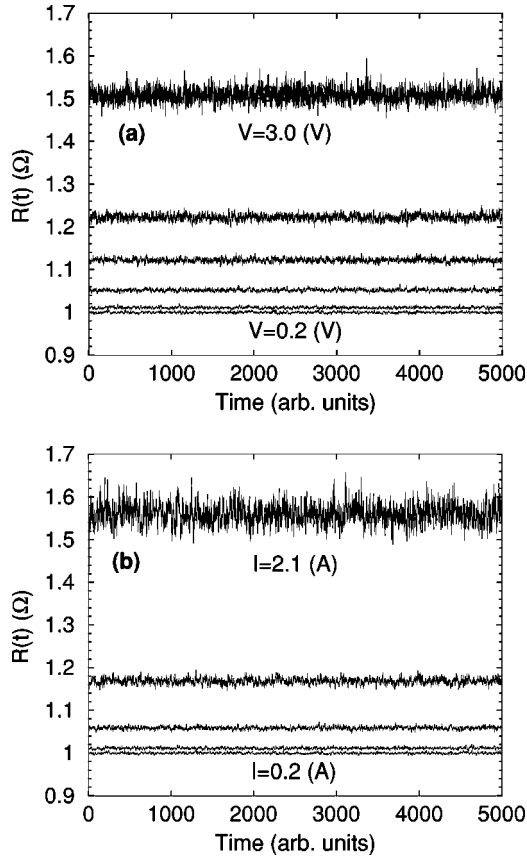


FIG. 1. (a) Resistance evolutions of a steady-state 75×75 network under constant-voltage conditions for increasing values of the bias. Going from the lower to the upper curves, the voltage is $V = 0.2, 0.5, 1.0, 1.5, 2.0,$ and 3.0 V. The values of all the other parameters are specified in the text. (b) Resistance evolutions of a steady-state 75×75 network under constant-current conditions for increasing values of the bias. Going from the lower to the upper curves, the current is: $I = 0.2, 0.5, 1.0, 1.5,$ and 2.1 A. The values of all the other parameters are specified in the text.

shown in these figures. Precisely, the RRN becomes unstable under constant voltage already by applying a voltage just above 3.0 V and, under constant current, by applying a current just above 2.1 A.

In the following, Figs. 2–4 will detail the behavior of the average resistance while Figs. 5–10 will focus on the results of resistance fluctuations.

A. Resistance

Figure 2 reports the average value of the RRN resistance as a function of the applied bias (current or voltage). Each value is calculated by considering the time average on a single steady-state realization and then averaging over 20 independent realizations (RRNs subjected to the same bias conditions). The numerical uncertainty is found to be within 0.01% at worst. At the lowest biases the resistance takes a value $\langle R \rangle_0$ that represents the intrinsic linear response property of the network (Ohmic regime) [42]. We note that for the activation energy values here chosen, the average fraction of defects at the lowest bias $\langle p \rangle_0$ is very small ($\langle p \rangle_0$

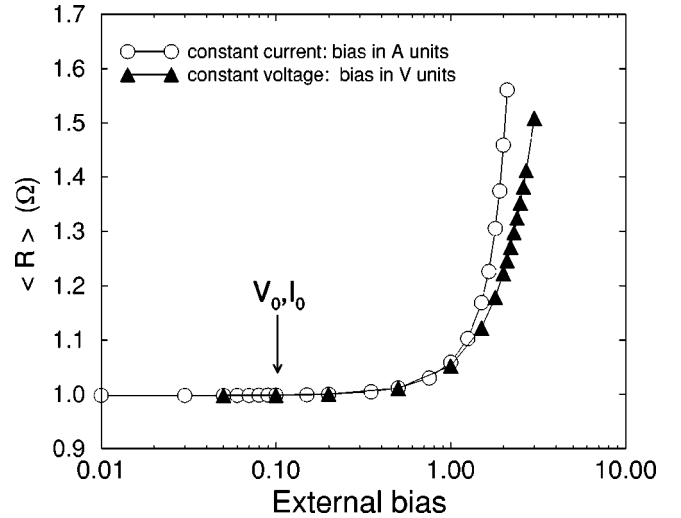


FIG. 2. Average network resistance as a function of the external bias. The averages are calculated over 20 networks of sizes 75×75 subjected to the same bias conditions. The circles correspond to biasing the network by an external constant current, the triangles correspond to a constant-voltage bias.

$= 0.545 \times 10^{-2}$) so that $\langle R_0 \rangle = 0.9978 \Omega$ is about 1% greater than the perfect network resistance. Under constant-current conditions, when the current overcomes a certain value I_0 the average resistance starts to become dependent on the bias. Thus, I_0 sets the current scale value for the onset of nonlinearity. By adopting as criterium for the onset of nonlinearity a resistance increase of 0.05% over the linear response value, we determine $I_0 = 0.090 \pm 0.005$ A. For currents above I_0 the resistance increase is smooth at moderate bias and it exhibits a sharp ramp (typical of a catastrophic behavior) at high bias, until a threshold current value $I_b = 2.10$ A above which the RRN undergoes an irreversible breakdown. A step of current values $\delta I = 0.05$ A has been used to determine I_b , thus this value of δI gives the maximum uncertainty on I_b . Accordingly, we have found $I_b/I_0 = 23 \pm 1$ and $\langle R \rangle_b / \langle R \rangle_0 = 1.6 \pm 0.1$, where $\langle R \rangle_b$ is the last stable value of the resistance calculated before the breakdown. We remark that the uncertainty on the ratio $\langle R \rangle_b / \langle R \rangle_0$ is mainly due to the uncertainty on $\langle R \rangle_b$ which reflects, amplified by the nonlinearity, the uncertainty on I_b . Similarly, under constant-voltage conditions we have found $V_b/V_0 = 32 \pm 2$ and $\langle R \rangle_b / \langle R \rangle_0 = 1.5 \pm 0.1$, where $V_0 = 0.095 \pm 0.005$ V and $V_b = 3.00$ V are the voltage values corresponding respectively to the nonlinearity onset and to the electrical breakdown. The maximum uncertainty on V_b is $\delta V = 0.05$ V. The significantly higher value of the ratio V_b/V_0 , when compared with that of the ratio I_b/I_0 , is a quantitative indication that the system is more robust when biased under constant-voltage than under constant-current conditions. This property is further emphasized by the fact that the increase of the resistance in the prebreakdown region exhibits a lower slope under constant-voltage than under constant-current conditions. It must be noticed that in spite of the significant difference of the ratios V_b/V_0 and I_b/I_0 , the ratio $\langle R \rangle_b / \langle R \rangle_0$ remains the same, within the error, under the different bias conditions. This

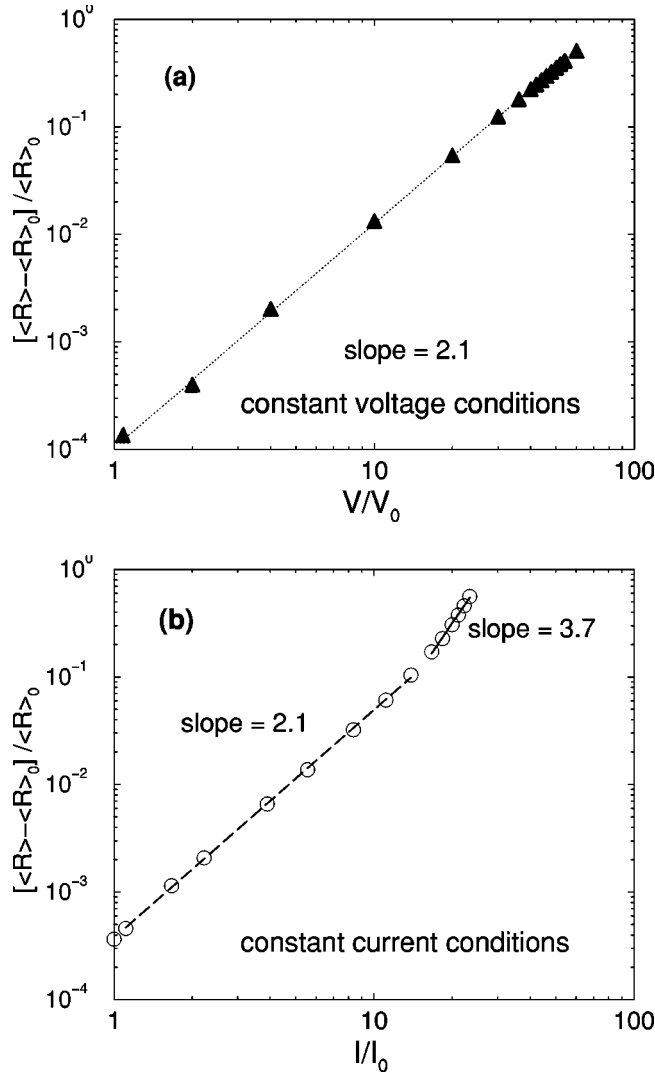


FIG. 3. (a) Log-log plot of the relative variation of the network resistance calculated under constant voltage as a function of the ratio V/V_0 . The data are the same of those in Fig. 2 and only the nonlinear regime is shown. The dotted line represents the power-law fit with a value for the exponent $\theta=2.1\pm 0.1$. (b) Log-log plot of the relative variation of the network resistance calculated under constant current as a function of the ratio I/I_0 . The data are the same of those in Fig. 2 and only the nonlinear regime is shown. The long-dashed line represents the power-law fit of the data in the moderate bias region, the value of the exponent is $\theta=2.1\pm 0.1$. The solid line fits the data in the prebreakdown region with a power law, the value of the exponent is $\theta_I=3.7\pm 0.1$.

result agrees with measurements of the ratio $\langle R \rangle_b / \langle R \rangle_0$ performed in composites under the Joule regime [15].

To better analyze the dependence on the bias of the average resistance, Figs. 3(a) and 3(b) report the log-log plot of the relative variation of the resistance as a function of V/V_0 and I/I_0 , respectively. Figure 3(a) shows that the relative variation of the average resistance scales with the ratio V/V_0 in the whole region of applied voltages up to breakdown as

$$\frac{\langle R \rangle_V}{\langle R \rangle_0} = 1 + a \left(\frac{V}{V_0} \right)^\theta, \quad (3)$$

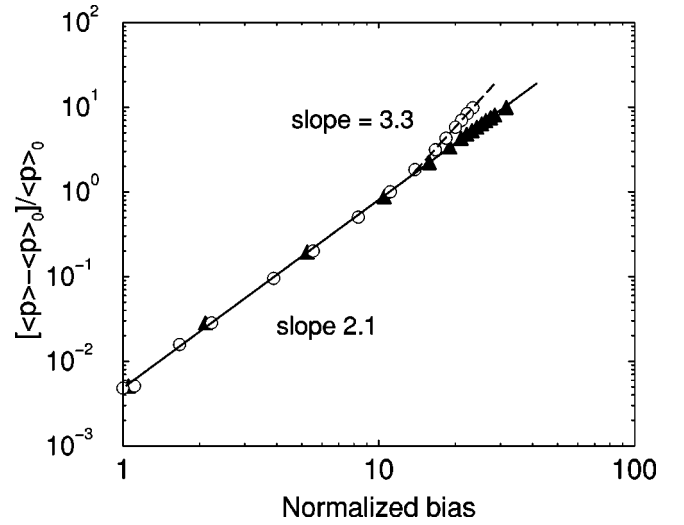


FIG. 4. Log-log plot of the relative variation of the average number of defects under constant-voltage (triangles) and under constant-current conditions (open circles) as a function of the normalized bias (V/V_0 or I/I_0). The solid line represents the power-law fit with a value for the exponent $\theta=2.1\pm 0.1$. The long-dashed line fits constant-current data in the prebreakdown region with a power law of exponent 3.3 ± 0.1 .

where $a=(1.1\pm 0.1)\times 10^{-4}$ is a dimensionless coefficient and $\theta=2.1\pm 0.1$. Figure 3(b) shows that also under constant current the relative variation of the average resistance scales with the ratio I/I_0 in the moderate bias region, as

$$\frac{\langle R \rangle_I}{\langle R \rangle_0} = 1 + a' \left(\frac{I}{I_0} \right)^\theta \quad (4)$$

with $a'=(3.8\pm 0.1)\times 10^{-4}$ and the same exponent θ of Eq. (3), within numerical uncertainty. However, in this case we notice that in the prebreakdown region the relative variation

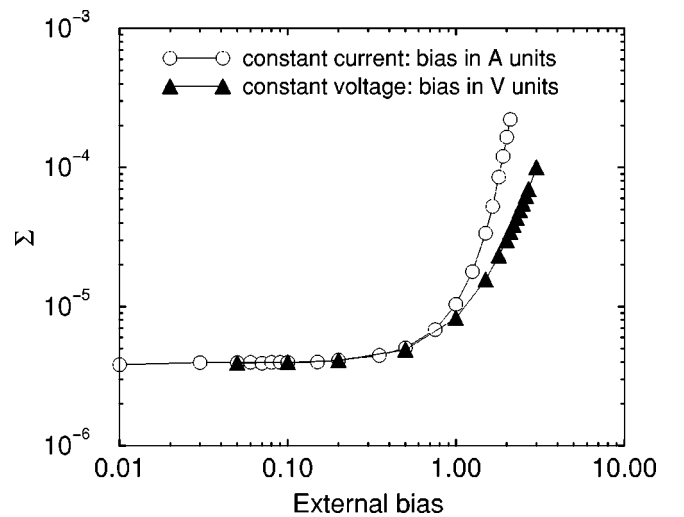


FIG. 5. Relative variance of resistance fluctuations Σ under constant-voltage conditions (triangles) and under constant-current conditions (open circles) as a function of the external bias. Each point has been obtained by averaging the variances calculated for 20 networks of sizes 75×75 subjected to the same bias conditions.

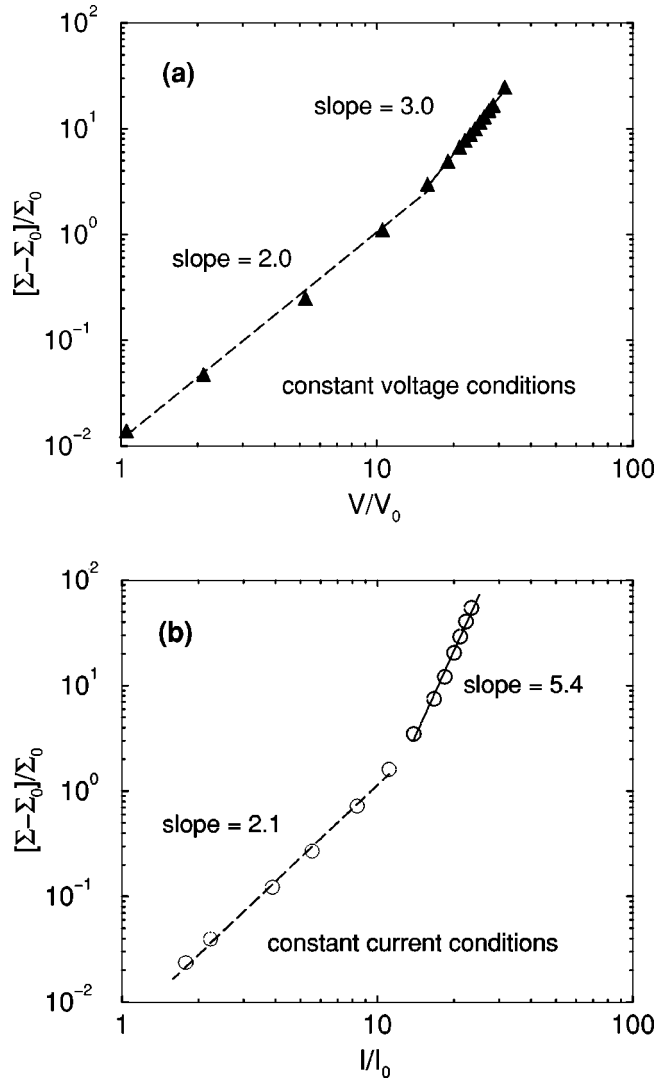


FIG. 6. (a) Log-log plot of the relative variation of Σ under constant-voltage conditions as a function of V/V_0 . The long-dashed line represents the power-law fit to the data in the moderate bias region, the value of the exponent is 2.0 ± 0.1 . The solid line fits data in the prebreakdown region with a power law of exponent 3.0 ± 0.1 . (b) Log-log plot of the relative variation of Σ under constant-current conditions as a function of I/I_0 . The long-dashed line represents the power-law fit to the data in the moderate bias region, the value of the exponent is 2.1 ± 0.1 . The solid line fits data in the prebreakdown region with a power law of exponent 5.4 ± 0.1 .

of the average resistance exhibits a superquadratic behavior characterized by a power law $(I/I_0)^{\theta_I}$ with $\theta_I = 3.7 \pm 0.1$.

This behavior of the average resistance with the applied bias can be understood as follows. From a macroscopic point of view, in a degradation process associated with a resistance increase, constant-current conditions lead, at increasing bias, to a superquadratic increase of the power dissipated through Joule heating and thus to a major efficiency in the defect generation. By contrast, constant-voltage conditions lead, at increasing bias, to a growth of the dissipated power which is subquadratic in the applied voltage, thus implying a minor efficiency in the generation of defects. In this respect, it must be underlined that the resistance increase driven by both kind

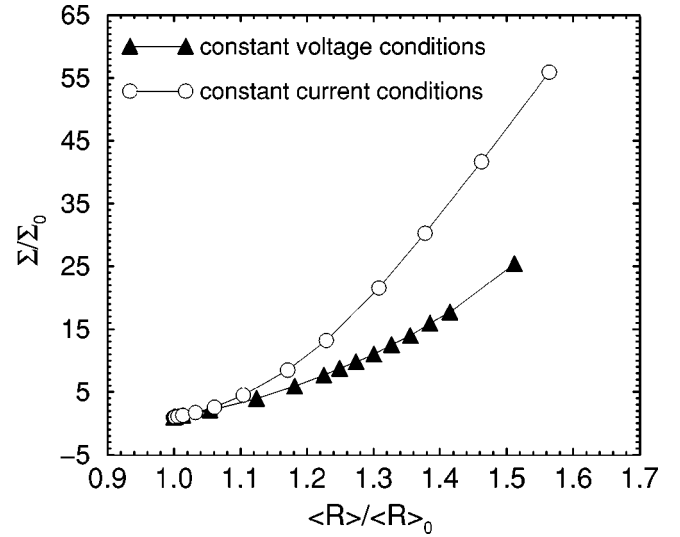


FIG. 7. Relative variance of resistance fluctuations normalized to the linear regime value as a function of the normalized average resistance. Open circles refer to constant-current condition and triangles to constant-voltage condition, respectively.

of bias is further enhanced by the positive value of the temperature coefficient of the resistance.

From a microscopic point of view, the RRN resistance depends on the average fraction of defects, $\langle p \rangle$, according to the expression [25]

$$\langle R \rangle \sim |\langle p \rangle - p_c|^{-\mu}, \quad (5)$$

where, for biased percolation, p_c and μ are functions of the bias strength [37,43]. Of course, for vanishing bias, p_c and μ take the well known values corresponding to random perco-

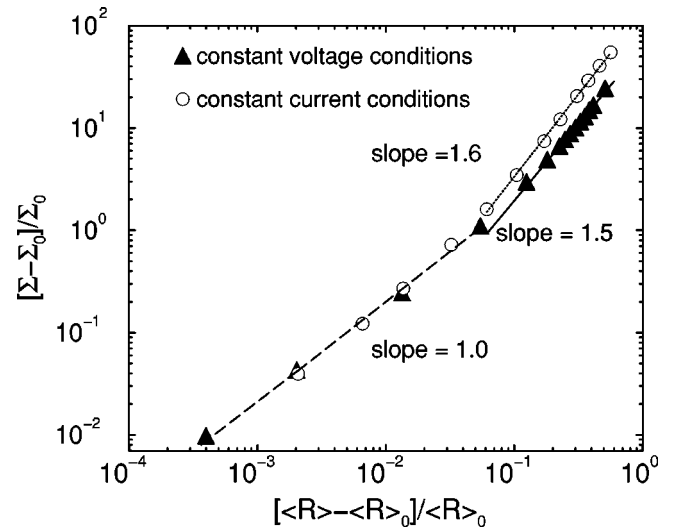


FIG. 8. Log-log plot of the relative variation of Σ as a function of the relative variation of the average resistance under constant-voltage condition (open circles) and constant-voltage condition (triangles). The long-dashed line gives the best fit with a power law with exponent 1.0 ± 0.1 . The solid and the dotted lines fit with a power law the data in the prebreakdown region, the exponents are 1.5 ± 0.1 and 1.6 ± 0.1 , respectively.

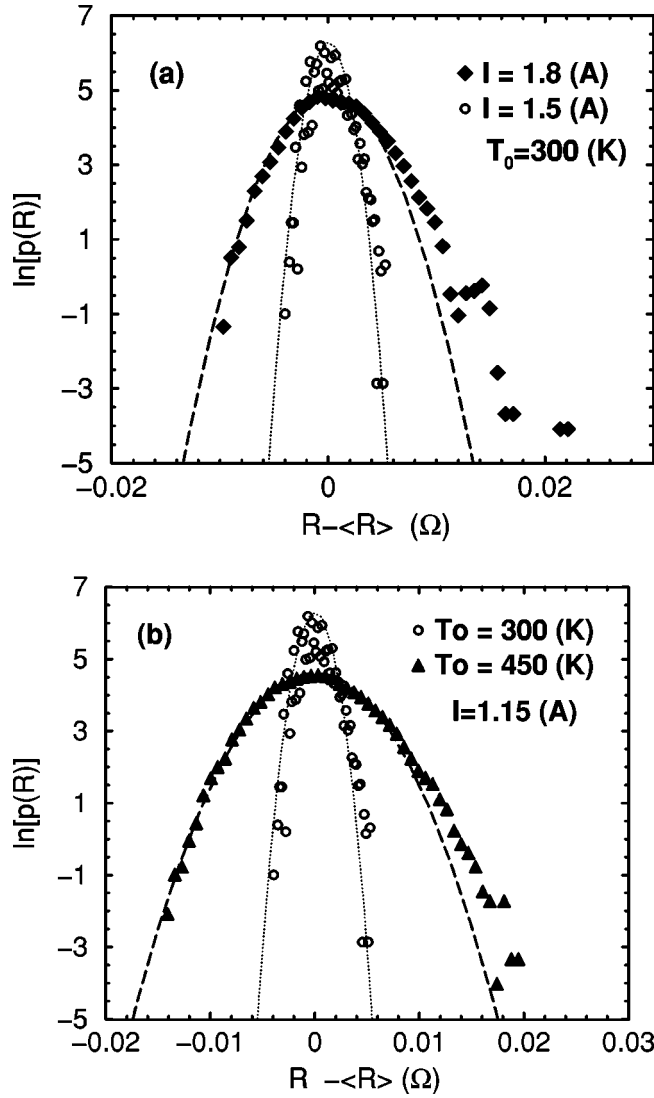


FIG. 9. (a) Distribution function of the resistance fluctuations for two values of the applied current. Open circles refer to $I = 1.5$ A and full diamonds to $I = 1.8$ A. The scale is a linear log, therefore, the dashed and the long-dashed curves, coming from parabolic fits of the two sets of data, correspond to Gaussian distributions. (b) Distribution function of the resistance fluctuations under constant-current conditions for two values of the substrate temperature. Open circles refer to $T_0 = 300$ K [the same data reported in Fig. 9(a)] and full triangles to $T_0 = 450$ K. The scale is linear log, therefore the dashed and the long-dashed curves, coming from parabolic fits of the two sets of data, correspond to Gaussian distributions.

lation: $p_c = 0.5$ (for a square lattice) and $\mu = 1.303$ (universal value) [25]. On the other hand, the dependence of p_c and μ on the bias makes the analysis of $\langle R \rangle$ in terms of Eq. (5) quite problematic. Nevertheless, it is interesting to analyze the behavior of $\langle p \rangle$ on the bias strength and, to this purpose, Fig. 4 reports on a log-log plot the relative variation of $\langle p \rangle$ as a function of the normalized bias. As evidenced by the figure, for the case of constant-voltage conditions the average fraction of defects scales with the same exponent θ over the full range of bias values, as

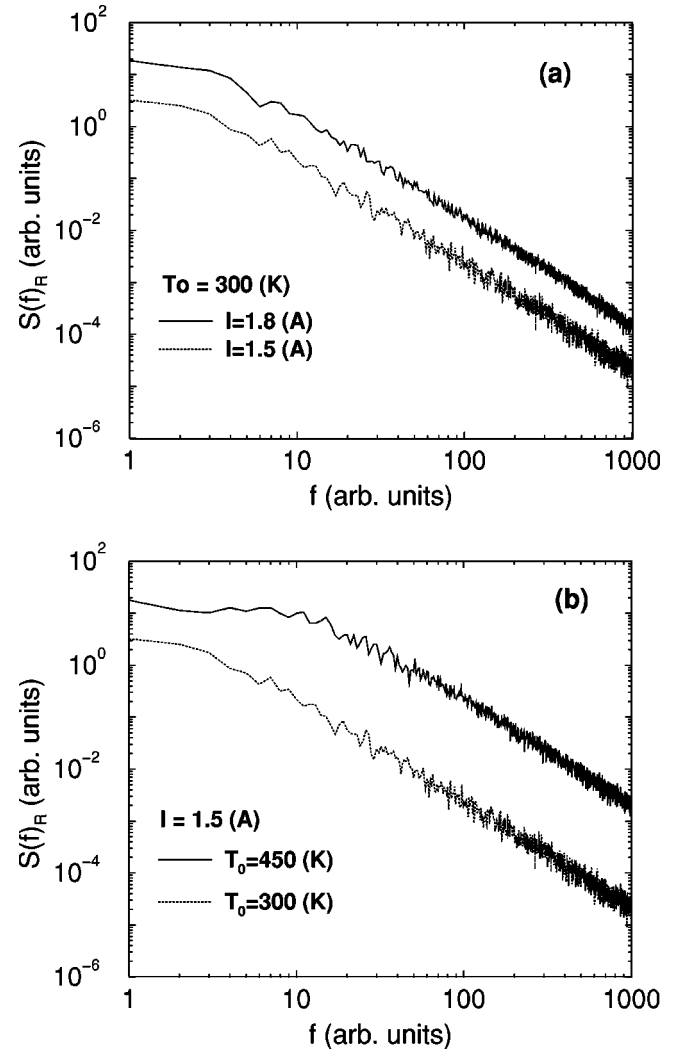


FIG. 10. (a) Power spectral density of resistance fluctuations under constant-current conditions for $I = 1.5$ A (dotted curve) and for $I = 1.8$ A (solid curve). In both cases the substrate temperature is 300 K. (b) Power spectral density of resistance fluctuations under constant-current condition for $T_0 = 300$ K (dotted curve) and for $T_0 = 450$ K (solid curve). In both cases the bias current is 1.5 A.

$$\frac{\langle p \rangle_V}{\langle p \rangle_0} = 1 + b \left(\frac{V}{V_0} \right)^\theta \quad (6)$$

with $b = (5.8 \pm 0.3) \times 10^{-3}$ a dimensionless coefficient. A similar expression holds under constant-current conditions at moderate bias,

$$\frac{\langle p \rangle_I}{\langle p \rangle_0} = 1 + b' \left(\frac{I}{I_0} \right)^\theta \quad (7)$$

with $b' = (5.3 \pm 0.3) \times 10^{-3}$. However, under constant current, there is a significant increase of the slope in the pre-breakdown region up to a nearly above cubic power law.

The behavior of the average fraction of defects in the moderate bias region can be understood by generalizing the results obtained in the case of two random processes [42] to the presence of a moderate external bias responsible for

Joule heating. In fact, for a RNN in a stationary state resulting from the competition of two random processes, it has been found [42] that $\langle p \rangle = x/(1+x)$, with $x = W_{0D}(1 - W_{0R})/W_{0R}$, where W_{0D} and W_{0R} are the probabilities defined in Sec. II with $T_n \equiv T_0$. At moderate bias, when the defect distribution is rather homogeneous and the variation of $\langle R \rangle$ small, we can take $x = x(T)$ with $T = T_0 + \Delta T$, where in the spirit of a mean-field theory, the average temperature increase can be expressed as $\Delta T = A \langle R \rangle_0 I^2 / (2N^2)$. Therefore, by differentiating,

$$\Delta \langle p \rangle = \frac{1}{(1+x)_0^2} \left(\frac{dx}{dT} \right)_0 \Delta T, \quad (8)$$

which by simple manipulation gives

$$\frac{\Delta \langle p \rangle}{\langle p \rangle_0} = \left[\frac{A \langle R \rangle_0 I_0^2}{2N^2 \langle p \rangle_0 [(1+x)^2]_0} \left(\frac{dx}{dT} \right)_0 \right] \left(\frac{I}{I_0} \right)^2. \quad (9)$$

The term in the squared brackets of Eq. (9) can thus be identified with the b' coefficient in Eq. (7). In fact, by introducing the parameters used in the simulations we find for the squared brackets in Eq. (9) the value 5.5×10^{-3} which well agrees with the previous reported value of b' . For constant voltage the factor $A \langle R \rangle_0 I_0^2$ inside Eq. (9) must be replaced with $A V_0^2 / \langle R \rangle_0$. This gives for the square bracket in Eq. (9) the value of 6.1×10^{-3} , which again well agrees with the value of b in Eq. (6). Therefore, at moderate bias, the quadratic behavior of $\langle p \rangle$ is well explained by Eq. (9). In the prebreakdown region, under constant-current conditions, the significant increase of the resistance and the defect filamentation characteristic of biased percolation [37,43] add to give a superquadratic increase of $\langle p \rangle$ with the bias. By contrast, under constant voltage, these two effects act in an opposed manner, thus their compensation results in a quadratic dependence of $\langle p \rangle$ over the full range of bias values.

From the above behavior of the average defect fraction we can now understand the bias dependence of $\langle R \rangle$. At moderate bias (I/I_0 or $V/V_0 \leq 10$) the increase of $\langle R \rangle$ is rather small. Accordingly, super and subquadratic effects on the dissipated power are negligible and the average fraction of defects over the intrinsic value grows quadratically with the bias strength [Eq. (9)]; at these bias values $\langle p \rangle \ll 1$ thus $\langle R \rangle \propto \langle p \rangle$ and also the average resistance grows quadratically with bias. At high bias (i.e., I/I_0 or $V/V_0 > 10$), when entering the prebreakdown region, the increase of $\langle R \rangle$ is significant. Accordingly, super and subquadratic effects on the dissipated power are relevant as well as the increase of the average fraction of defects, which now takes a nonuniform distribution (biased percolation). As a consequence, the percolation threshold is lowered with respect to the random percolation value [43]. Depending on constant-current or constant-voltage conditions, this biased percolation effect adds to further enhancing the increase of the resistance well above the quadratic law or to keep the quadratic behavior, respectively.

This interpretation is confirmed by MC simulations performed with the same parameters but setting the temperature

coefficient of the resistance $\alpha = 0$. In this case, we have found that the onset of nonlinearity as well as the electrical breakdown occur at higher values of the bias. Precisely we have found $I'_0 = 0.25 \pm 0.03$ A, $I'_b = 2.65 \pm 0.05$ A (thus $I'_b/I'_0 = 11 \pm 1$), $\langle R \rangle_b / \langle R \rangle_0 = 1.2 \pm 0.1$ under constant-current and $V'_0 = 0.25 \pm 0.03$ V, $V'_b = 3.25 \pm 0.05$ V (thus $V_b/V_0 = 13 \pm 1$), and $\langle R \rangle_b / \langle R \rangle_0 = 1.3 \pm 0.1$ under constant-voltage conditions. The quadratic regime is always present at moderate bias values. However, in the prebreakdown regime we have found $\theta'_I = 3.1 \pm 0.1$ for constant-current and $\theta'_V = 2.8 \pm 0.1$ for constant-voltage conditions, respectively.

We finally conclude this section by remarking that the behavior described by Eqs. (3) and (4) well agrees with measurements of the resistance of composites made in the Joule regime up to breakdown [15].

B. Fluctuations

It is well known that important information about the properties and the stability of different systems (physical, biological, social, etc.) can be obtained by studying the fluctuations around the average value of some characteristic quantities of the system [1–3,14–20,28–31,33–45]. Several features of the fluctuations are usually considered, and among these, the most important are the variance (or the relative variance), the power spectrum and the Gaussianity property. Here, we analyze the fluctuations of the RNN resistance in the full range of bias values, devoting particular attention to the features that can be identified as failure precursors. Figure 5 reports the relative variance of resistance fluctuations, $\Sigma \equiv \langle \delta R^2 \rangle / \langle R \rangle^2$, as a function of the applied bias. The data correspond to the same simulations presented in Fig. 2. The same procedure of time averaging over a single simulation and then making ensemble averages over 20 realizations provides an uncertainty of 3% at worst. At low bias, the relative variance is found to achieve a constant value $\Sigma_0 = (4.0 \pm 0.1) \times 10^{-6}$. This value represents an intrinsic property of the system determined by the competition of two random processes, as already discussed for the case of the resistance. A detailed analysis of the scaling properties of Σ_0 can be found in Ref. [42]. At increasing bias, when $I > I_0$ or $V > V_0$, the systematic increase of Σ reveals the existence of a nonlinear regime of the response. Similarly to the behavior of the resistance, by approaching the electrical breakdown Σ exhibits a significant increase that is steeper under constant-current than under constant-voltage conditions. This feature is ascribed to the better stability of the RNN under constant voltage, since resistance fluctuations in excess over the mean value are damped in this condition. By contrast, the same kind of fluctuations are enhanced under constant-current conditions. To detail the dependence of Σ on the bias, we have reported in Fig. 6(a) its relative variation, $[\Sigma_V - \Sigma_0] / \Sigma_0$, as a function of V/V_0 under constant-voltage conditions. Two regions can be identified in the nonlinear regime: a moderate bias region ($V/V_0 < 10$), characterized by a quadratic dependence on the applied voltage, and a prebreakdown region at the highest voltages

($V/V_0 > 10$), where a superquadratic dependence up to a cubic power law is evidenced. Accordingly, in the first region it is

$$\frac{\Sigma_V}{\Sigma_0} = 1 + c \left(\frac{V}{V_0} \right)^2 \quad (10)$$

with $c = (1.14 \pm 0.06) \times 10^{-2}$ a dimensionless coefficient, while in the second region we have found

$$\frac{\Sigma_V}{\Sigma_0} \sim \left(\frac{V}{V_0} \right)^{\eta_V}, \quad (11)$$

where $\eta_V = 3.0 \pm 0.1$. This behavior of Σ under constant-voltage conditions should be compared with that of the average resistance that remains always a quadratic function up to the breakdown, as shown in Fig. 3(a). The emergence of a superquadratic behavior of Σ in the prebreakdown region reflects the higher sensitivity of the resistance fluctuations with respect to the average value of the resistance to the instability of the network. The same analysis performed for the case of constant current is shown in Fig. 6(b). Again, at moderate bias $[\Sigma_I - \Sigma_0]/\Sigma_0$ increases quadratically with the current as

$$\frac{\Sigma_I}{\Sigma_0} = 1 + c' \left(\frac{I}{I_0} \right)^2 \quad (12)$$

with $c' = (6.6 \pm 0.4) \times 10^{-3}$ a dimensionless coefficient. On the other hand, the superquadratic dependence characterizes the prebreakdown region as

$$\frac{\Sigma_I}{\Sigma_0} \sim \left(\frac{I}{I_0} \right)^{\eta_I} \quad (13)$$

with $\eta_I = 5.4 \pm 0.1$. We note, that η_I is significantly greater than η_V , according to the behaviors shown in Fig. 5. Moreover, η_I is greater than the resistance exponent in the prebreakdown region θ_I . It is noteworthy, that by neglecting the effect of the temperature coefficient of the resistance, i.e., by taking $\alpha = 0$, the moderate bias region remains characterized by a quadratic increase that is common to both constant-current and constant-voltage conditions. However, in the prebreakdown region we have found $\eta_V = \eta_I = 4.0 \pm 0.1$. Thus, the above results prove that the quadratic dependence of Σ on the bias in the moderate bias region is a feature independent of the conditions on which the bias is applied and also independent of the value of the thermal coefficient of the resistance. This reflects the fact that at moderate bias the two following conditions are satisfied: (i) the variation of the average fraction of defects follows Eq. (9); (ii) the average fraction of defects is much smaller than the percolation threshold value, i.e., $\langle p \rangle \ll p_c$. Therefore, in this nearly perfect regime $\Sigma \propto \langle p \rangle \propto \langle R \rangle$ [42]. On the other hand, the superquadratic behavior of Σ in the prebreakdown region is a consequence of the fact that at high biases the local correlations in the defect generation and recovery processes become strong. Defect filamentation, characteristic of biased percola-

tion [37,43], implies that a small variation in the number of defects bring strong resistance fluctuations.

Figure 7 reports the relative variance of resistance fluctuations normalized to the linear regime value as a function of the normalized resistance. Constant-current (open circles) and constant-voltage (full triangles) conditions are shown. We can see that the former quantity increases of more than one order of magnitude in the same range of bias values where the latter quantity increases for about 60% only. The log-log plot of $[\Sigma - \Sigma_0]/\Sigma$ as a function of $[\langle R \rangle - \langle R \rangle_0]/\langle R \rangle_0$, shown in Fig. 8 under both bias conditions, confirms the proportionality of Σ with $\langle R \rangle$ in the moderate bias region and evidences the following power law in the prebreakdown region:

$$\frac{[\Sigma - \Sigma_0]}{\Sigma_0} \sim \frac{[\langle R \rangle - \langle R \rangle_0]^\zeta}{\langle R \rangle_0}, \quad (14)$$

where the value of the exponent $\zeta = 1.5 \pm 0.1$, is practically the same (within the statistical uncertainty) for constant-voltage or constant-current conditions. This result is consistent with Eqs. (3) and (4).

To complete the study of resistance fluctuations, we have investigated the Gaussian properties of the fluctuation amplitudes and the spectra in the frequency domain. Figures 9(a) and 9(b) report the distribution function of the resistance fluctuations $p(R)$ for different currents and different bath temperatures, respectively. The dotted and the long-dashed curves in Fig. 9(a) correspond to fit with a Gaussian distribution the data corresponding to different current values in the prebreakdown region at $T_0 = 300$ K, while in Fig. 9(b) to fit the data corresponding to different bath temperatures at $I = 1.5$ A. When approaching the breakdown conditions, at increasing current in Fig. 9(a) and at increasing temperature in Fig. 9(b), the simulations show the onset of a non-Gaussian behavior characterized by the enhancement of the probability for the positive fluctuations with respect to the Gaussian distribution. The emergence of a non-Gaussian behavior near the breakdown, in agreement with experiments [45,40,41], can be considered a relevant precursor of failure.

Figures 10(a) and 10(b) show the spectral densities of resistance fluctuations for the same conditions of Figs. 9(a) and 9(b). The spectral densities have been calculated by Fourier transforming the corresponding correlation functions $C_{\delta R}(t)$. We have found Lorentzian spectra in all the cases. For a given temperature, within the numerical uncertainty, the corner frequency is found to be independent of the applied current, while the value of the plateau increases more than quadratically with the current in the prebreakdown region. For a given current in the prebreakdown region, both the corner frequency and the value of the plateau are found to increase at increasing temperatures. This fact indicates that the characteristic times of fluctuations while depending on temperature are independent of the applied bias. We finally remark that the power spectral density in Figs. 10(a) and 10(b) are in good agreement with experiments [17,19,45].

IV. CONCLUSIONS

We have studied the stationary state of a two-dimensional RRN resulting from the competition between two biased processes. The two processes consist of the breaking and recovering of elementary resistors and they are driven by the joint effects of an electrical bias and of the heat exchange with a thermal bath. The electrical bias is set up by applying a constant voltage or a constant current. MC simulations have been performed to analyze the network resistance and its fluctuation properties in the full range of bias values, covering linear and nonlinear regimes up to the breakdown limit. The nonlinear regime starts for biases greater than the threshold values, V_0 or I_0 (nonlinearity onset values), and it extends until the values V_b or I_b (breakdown values). The ratios V_b/V_0 , I_b/I_0 , $\langle R \rangle_b/\langle R \rangle_0$ can be considered as relevant indicators characterizing the breakdown properties of the system. We have found that the ratio $\langle R \rangle_b/\langle R \rangle_0$ is independent of the bias conditions but it depends on the thermal coefficient of the resistance. This result agrees with measurements of this ratio performed in composites [15]. Moreover, we have found that under constant-voltage conditions the relative variation of the average resistance scales quadratically with the ratio V/V_0 over the full nonlinear regime. A similar relation has been found under constant-current conditions, but in this case a superquadratic dependence emerges in the prebreakdown region ($I > 10I_0$). For what concerns the relative variance of resistance fluctuations we have found that at moderate bias ($I_0 < I < 10I_0$) it grows quadratically with the bias, independently of constant-current or constant-voltage conditions. On the other hand a superqua-

dratic dependence appears in the prebreakdown region. The presence of two distinct regions in the nonlinear regime has been explained in the following terms. At moderate bias there is a small Joule heating giving rise to the competitions of two nearly random processes and to a small variation of the RRN resistance. At high bias, local correlations typical of biased percolation become important. Moreover, also the resistance variation becomes strong. Therefore, as a consequence of both these effects the resistance noise depends superquadratically on the bias. The power spectral density of resistance fluctuations is found to exhibit a Lorentzian spectrum and in the prebreakdown region the amplitude of fluctuations shows the onset of non-Gaussian behaviors. Theoretical results agree qualitatively, and in some cases quantitatively, with breakdown experiments performed in composites [14,15] and in other conducting [17,20,40] or nonconducting materials [41]. We conclude that the study of the stationary state of a RRN, resulting from the competition of biased percolative processes, provides an unifying framework for the interpretation of several nonlinear transport phenomena in a variety of disordered systems.

ACKNOWLEDGMENTS

This research is performed within the STATE project of INFN. Partial support is also provided by the MADESS II project of the Italian National Research Council and the ASI project, Contract No. I/R/056/01. We thank Professor L. B. Kish and Dr. Z. Gingl who introduced us to the biased percolation picture.

-
- [1] H. J. Herrmann and S. Roux, *Statistical Models for the Fracture of Disordered Media* (North-Holland, Amsterdam, 1990).
- [2] K. K. Bardhan, B. K. Chakrabarti, and A. Hansen, *Non-Linearity and Breakdown in Soft Condensed Matter* (Springer-Verlag, New York, 1994).
- [3] A. Bunde and S. Havlin, *Fractals and Disordered Systems* (Springer-Verlag, Berlin, 1996).
- [4] L. De Arcangelis, A. Hansen, H. J. Herrmann, and S. Roux, *Phys. Rev. B* **40**, 877 (1989).
- [5] M. Sahimi and S. Arbabi, *Phys. Rev. Lett.* **68**, 608 (1992).
- [6] M. B. Heaney, *Phys. Rev. B* **52**, 12 477 (1995).
- [7] M. Acharyya and B. K. Chakrabarti, *Phys. Rev. E* **53**, 140 (1996).
- [8] J. V. Andersen, D. Sornette, and K. T. Leung, *Phys. Rev. Lett.* **78**, 2140 (1997).
- [9] S. Zapperi, A. Vespignani, and H. E. Stanley, *Nature (London)* **388**, 659 (1997); S. Zapperi, P. Ray, H. E. Stanley, and A. Vespignani, *Phys. Rev. Lett.* **78**, 1408 (1997); *Physica A* **270**, 57 (1999).
- [10] R. Albert, H. Jeong, and A. L. Barabasi, *Nature (London)* **406**, 378 (2000); A. L. Barabasi and R. Albert, *Science* **286**, 509 (1999).
- [11] A. Gabrielli, G. Caldarelli, and L. Pietronero, *Phys. Rev. E* **62**, 7638 (2000).
- [12] R. K. Chakrabarti, K. K. Bardhan, and A. Basu, *Phys. Rev. B* **44**, 6773 (1991); K. K. Bardhan, *Physica A* **241**, 267 (1997).
- [13] L. Lemaître, F. Carmona, and D. Sornette, *Phys. Rev. Lett.* **77**, 2738 (1996).
- [14] U. N. Nandi, C. D. Mukherjee, and K. K. Bardhan, *Phys. Rev. B* **54**, 12 903 (1996).
- [15] C. D. Mukherjee, K. K. Bardhan, and M. B. Heaney, *Phys. Rev. Lett.* **83**, 1215 (1999).
- [16] Z. Rubin, S. A. Sunshine, M. B. Heaney, I. Bloom, and I. Balberg, *Phys. Rev. B* **59**, 12 196 (1999).
- [17] A. Scorzoni, B. Neri, C. Caprile, and F. Fantini, *Mater. Sci. Rep.* **7**, 143 (1991).
- [18] B. K. Jones, Y. Z. Xu, and P. Zobbi, *Microelectron. Reliab.* **36**, 1051 (1996).
- [19] M. Ohring, *Reliability and Failure of Electronic Materials and Devices* (Academic Press, San Diego, 1998).
- [20] I. Bloom and I. Balberg, *Appl. Phys. Lett.* **74**, 1427 (1999).
- [21] S. Hirano and A. Kishimoto, *Jpn. J. Appl. Phys., Part 2* **38**, L662 (1999).
- [22] L. B. Kish, P. Chaoguang, J. Ederth, C. G. Granqvist, and S. J. Savage, *Surf. Coat. Technol.* (to be published).
- [23] C. Pennetta, L. Reggiani, G. Trefan, F. Fantini, A. Scorzoni, and I. De Munari, *J. Phys. D* **34**, 1421 (2001).
- [24] H. E. Stanley, *Rev. Mod. Phys.* **71**, S358 (1999).
- [25] D. Stauffer and A. Aharony, *Introduction to Percolation Theory* (Taylor & Francis, London, 1992).

- [26] M. Sahimi, *Application of Percolation Theory* (Taylor & Francis, London, 1994).
- [27] P. M. Duxbury, P. L. Leath, and P. D. Beale, *Phys. Rev. B* **36**, 367 (1987).
- [28] R. Rammal, C. Tannous, P. Breton, and A. M. S. Tremblay, *Phys. Rev. Lett.* **54**, 1718 (1985); R. Rammal, C. Tannous, and A. M. S. Tremblay, *Phys. Rev. A* **31**, 2662 (1985).
- [29] R. Rammal and A. M. S. Tremblay, *Phys. Rev. Lett.* **58**, 415 (1987).
- [30] M. A. Dubson, Y. C. Hui, M. B. Weissman, and J. C. Garland, *Phys. Rev. B* **39**, 6807 (1989).
- [31] Y. Yagil, G. Deutscher, and D. J. Bergman, *Phys. Rev. Lett.* **69**, 1423 (1992); Y. Yagil and G. Deutscher, *Phys. Rev. B* **46**, 16 115 (1992).
- [32] D. Sornette and C. Vanneste, *Phys. Rev. Lett.* **68**, 612 (1992).
- [33] A. A. Snarskii, A. E. Morozovsky, A. Kolek, and A. Kusy, *Phys. Rev. E* **53**, 5596 (1996).
- [34] A. Gingl, C. Pennetta, L. B. Kish, and L. Reggiani, *Semicond. Sci. Technol.* **11**, 1770 (1996).
- [35] I. Balberg, *Phys. Rev. B* **57**, 13 351 (1998).
- [36] C. Pennetta, L. Reggiani, and L. B. Kish, *Physica A* **266**, 214 (1999).
- [37] C. Pennetta, L. Reggiani, and Gy. Trefan, *Phys. Rev. Lett.* **84**, 5006 (2000).
- [38] C. Pennetta, Gy. Trefan, and L. Reggiani, in *Proceedings of the Second International Conference in Unsolved Problems of Noise and Fluctuations*, edited by D. Abbott and L. B. Kish (AIP, New York, 1999), p. 447.
- [39] C. Pennetta, E. Alfinito, L. Reggiani, and G. Trefan, *J. Phys. C* **14**, 2371 (2002).
- [40] G. T. Seidler, S. A. Solin, and A. C. Marley, *Phys. Rev. Lett.* **76**, 3049 (1996).
- [41] N. Vandewalle, M. Ausloos, M. Houssa, P. W. Mertens, and M. M. Heyns, *Appl. Phys. Lett.* **74**, 1579 (1999).
- [42] C. Pennetta, G. Trefan, and L. Reggiani, *Phys. Rev. Lett.* **85**, 5238 (2000).
- [43] C. Pennetta, L. Reggiani, and G. Trefan, *Math. Comput. Simul.* **55**, 231 (2001).
- [44] Y. C. Zhang, *Phys. Rev. B* **36**, 2345 (1987).
- [45] M. B. Weissman, *Rev. Mod. Phys.* **60**, 537 (1988).